Journal of Agricultural Sciences Research

ISSN 2764-0973 vol. 6, n. 3, 2026

ARTICLE 5

Data de Aceite: 07/07/2026

FROM BLOCK FREEZE CONCENTRATION BY-PRODUCT TO ACTIVE BIODEGRADABLE PACKAGING: UTILIZATION OF THE ICE FRACTION FROM *PINHÃO* FAILURE EXTRACT

Ana Caroline Ferreira Carvalho
Postgraduate Program in Food Engineering, Technology Center, Federal University of Santa Catarina, Trindade, Florianopolis, SC, Brazil
Department of Chemical Engineering, University of Blumenau, São Paulo Street, Blumenau, SC, Brazil

Karine Marafon
Postgraduate Program in Food Engineering, Technology Center, Federal University of Santa Catarina, Trindade, Florianopolis, SC, Brazil
Department of Chemical, Pharmaceutical and Agricultural Sciences, University of Ferrara, Ferrara, Italy

Amanda Alves Prestes
Postgraduate Program in Food Engineering, Technology Center, Federal University of Santa Catarina, Trindade, Florianopolis, SC, Brazil

Julia Prebianca
Postgraduate Program in Chemical Engineering, University of Blumenau, São Paulo Street, Blumenau, SC, Brazil

Dayanne Regina Mendes Andrade
Postgraduate Program in Food Engineering, Federal University of Parana, Jardim das Americas, Curitiba, PR, Brazil

Cristiane Vieira Helm
Brazilian Agricultural Research Corporation (Embrapa Florestas), Guaraituba, Colombo, PR, Brazil

Jefferson Santos de Gois
Department of Analytical Chemistry, Rio de Janeiro State University, Rio de Janeiro, RJ, Brazil

Paola Tedeschi
Department of Chemical, Pharmaceutical and Agricultural Sciences, University of Ferrara, Ferrara, Italy

Carolina Krebs de Souza
Postgraduate Program in Chemical Engineering, University of Blumenau, São Paulo Street, Blumenau, SC, Brazil
Department of Chemical Engineering, University of Blumenau, São Paulo Street, Blumenau, SC, Brazil

Elane Schwinden Prudêncio
Postgraduate Program in Food Engineering, Technology Center, Federal University of Santa Catarina, Trindade, Florianopolis, SC, Brazil
Department of Food Science and Technology, Federal University of Santa Catarina, Itacorubi, Florianópolis, SC, Brazil

Abstract: The ice fraction generated during block freeze concentration is commonly regarded as a low-value by-product despite retaining appreciable amounts of bioactive compounds. This study investigated the use of the ice fraction (I2) obtained from the second stage of block freeze concentration of *Pinhão* failure (*Araucaria angustifolia*) extract as a functional additive in biodegradable starch/carboxymethylcellulose (CMC) films. The block freeze concentration process showed progressive enrichment of gallic acid, with concentration factors of 9.90, 22.13, and 22.50 for C1, C2, and C3, respectively. The second concentration stage exhibited the highest process efficiency (53.54%), and its ice fraction (I2) was selected for film production. Films containing I2 (FI2) exhibited lower thickness and moisture content than the control film, while presenting higher water vapor permeability and contact angle values. The incorporation of I2 significantly improved tensile strength and elongation at break without affecting Young's modulus. FTIR analysis suggested intermolecular interactions between compounds retained in the ice fraction and the polymeric matrix, while SEM micrographs revealed a continuous and homogeneous structure. FI2 also exhibited antioxidant activity and pH-responsive color changes, indicating potential application as an active and intelligent packaging material. Although the incorporation of I2 slightly delayed biodegradation, complete degradation was achieved within 42 days under soil burial conditions. These results demonstrate that the ice fraction recovered from block freeze concentration can be successfully valorized as a functional ingredient for the development of sustainable biodegradable packaging materials.

Keywords: *Araucaria angustifolia*, block freeze concentration, ice fraction valorization, biodegradable film, smart packaging, circular economy

Highlights:

- The ice fraction from block freeze concentration of *Pinhão* failure extract was successfully valorized.
- The second freeze concentration stage showed the highest process efficiency (53.54%).
- Incorporation of I2 improved tensile strength and elongation at break of starch–CMC films.
- FI2 films exhibited antioxidant activity and pH-responsive behavior, indicating a smart packaging property.
- Complete biodegradation occurred within 42 days under soil burial conditions.

INTRODUCTION

The ongoing demand for sustainable food systems has intensified the search for strategies that simultaneously reduce agro-industrial waste and develop environmentally friendly food packaging materials. In this context, the valorization of agricultural by-products is an important pillar of circular economy principles, contributing to efficient resource use and minimizing waste generation (Carvalho, Ghosh, et al., 2025).

*Araucaria angustifoli*a (Bertol.) Kuntze, commonly known as the Brazilian pine, is a native tree species of great ecological, cultural, and economic importance in Southern Brazil. Its seeds, known as *Pinhão,* are widely consumed for their nutritional value and used in both traditional and industrial food products (Finger et al., 2023). However, the processing and commercialization of *pinhão* generate considerable amounts of by-products, including fractions that do not meet commercial quality standards. Depending on harvesting, processing, and sorting conditions, a substantial proportion of seeds may be discarded due to physical damage, irregular size, or defects that reduce their market acceptance. The underutilization of these fractions represents not only an economic loss but also an environmental challenge associated with agro-industrial residue management (Marafon et al., 2025). These materials, commonly referred to as *pinhão* failures (non-commercial *pinhão* fractions), consist of fragmented kernels, mechanically damaged seeds, irregularly sized fractions, and units with physical defects that limit their direct commercialization. Despite their reduced market value, these fractions still contain significant amounts of nutrients and bioactive compounds, highlighting the need for sustainable alternatives for their utilization (Nolasco et al., 2024).

Previous studies have demonstrated that *pinhão* by-products are rich sources of phenolic compounds, antioxidants, and other bioactive metabolites with potential applications in food, pharmaceutical, and packaging industries (Salvadori et al., 2024). These compounds are associated with antioxidant activity and may contribute to the development of active materials with enhanced functionality (Sbruzzi Fiebig et al., 2024). Phenolic compounds can act as natural radical scavengers, delaying oxidative reactions in food systems and potentially extending product shelf life when incorporated into packaging materials. Further-

more, these compounds may interact with polymeric matrices, influencing film structure and functionality (Asrafali et al., 2026; Cazón et al., 2025). Nevertheless, the direct use of *pinhão* failure fractions is limited by their high moisture content and susceptibility to physicochemical and microbiological degradation. Consequently, preservation technologies that can concentrate and protect thermolabile compounds are required to maximize their technological value.

Among emerging concentration technologies, block freeze concentration (BFC) has attracted considerable attention as a sustainable alternative to conventional thermal evaporation processes (Prestes et al., 2022). BFC is based on the controlled freezing of a liquid matrix followed by the separation of the concentrated liquid phase from the ice fraction. Because water crystallizes preferentially during freezing, solutes become concentrated in the unfrozen phase. Compared with thermal concentration methods, BFC operates at low temperatures, minimizing the degradation of heat-sensitive compounds and preserving nutritional, sensory, and functional characteristics (Carvalho et al., 2026; Marafon et al., 2024). This technology has been successfully applied to fruit juices, plant extracts, coffee, wine, and functional beverages, demonstrating its effectiveness in concentrating bioactive compounds while maintaining product quality (Casas-Forero et al., 2020; Moreno et al., 2014; Vilar-Bustillo et al., 2023).

Traditionally, the ice fraction generated during freeze concentration is considered a secondary by-product and is frequently discarded. However, several studies have shown that some soluble solids, phenolic compounds, and antioxidant molecules may remain entrapped within the ice matrix during freezing (Pérez-Bermúdez et al., 2025). Its exploitation may therefore help maximize raw material utilization while enhancing the sustainability and economic viability of freeze concentration processes. This finding suggests that the ice fraction may still possess technological and functional value, creating opportunities for its utilization rather than disposal. Such an approach aligns with circular economy principles by promoting the complete use of raw materials and reducing process losses. Despite this potential, studies investigating the technological applications of ice fractions obtained from freeze concentration processes remain scarce, particularly for agro-industrial by-products.

The retention of bioactive compounds within the ice fraction is influenced by the freezing rate, solute composition, and crystal growth dynamics (Prestes et al., 2022). As a result, this fraction may contain appreciable amounts of phenolic compounds, antioxidants, pigments, and other phytochemicals that remain entrapped during ice formation (Pérez-Bermúdez et al., 2025). Rather than being considered a process residue, the ice fraction may represent a valuable secondary stream capable of providing functional properties for new biomaterials (Pérez-Bermúdez et al., 2025).

Simultaneously, growing environmental concerns regarding petroleum-based plastics have stimulated the development of biodegradable packaging materials derived from renewable resources (Pérez-Bermúdez et al., 2025). Starch-based films have emerged as promising alternatives due to their biodegradability, availability, low cost, and film-forming ability (Karnwal et al., 2025). The incorporation of carboxymethyl cellulose (CMC) can further improve the film's structure and mechanical performance by

enhancing polymer interactions (Beghetto et al., 2026). Moreover, the incorporation of plant-derived extracts and bioactive compounds into biodegradable matrices has enabled the development of active and intelligent packaging systems (Cazón et al., 2025). Phenolic compounds can provide antioxidant activity, reducing oxidative deterioration and contributing to food preservation, while naturally occurring pigments and other phytochemicals may confer responsiveness to environmental changes, allowing color modifications that can potentially serve as indicators of food quality and storage conditions (Asrafali et al., 2026). Such characteristics have stimulated growing interest in developing multifunctional packaging systems that simultaneously protect foods and provide information on product freshness and quality (Cazón et al., 2025).

Although freeze concentration has been extensively investigated as a method for recovering and concentrating valuable compounds from plant matrices (Uald-lamkaddam et al., 2021), the technological valorization of the ice fraction generated during this process remains largely unexplored. Most studies have focused on the concentrated liquid phase, while the potential functionality of compounds retained in the ice fraction has received limited attention. Furthermore, the use of ice fractions derived from cryoconcentrated agro-industrial by-products as functional additives in biodegradable packaging systems has not been systematically investigated. No studies have reported the use of the ice fraction obtained from cryoconcentrating *pinhão* failure extracts. Furthermore, little information is available on incorporating such fractions into biodegradable polymeric matrices for packaging applications. Understanding how this underexplored fraction influences the physical, mechanical, structural, antioxidant, and biodegradation properties of biodegradable films is essential for establishing new valorization routes for agro-industrial residues and advancing sustainable packaging technologies.

It was hypothesized that the ice fraction obtained from the block-freeze concentration of *pinhão* failure extract retains enough bioactive compounds to serve as a functional additive in starch/CMC biodegradable films. The incorporation of this fraction is expected to enhance the films' antioxidant properties while maintaining adequate structural, mechanical, and biodegradation performance, thereby creating an innovative route for the valorization of an underutilized agro-industrial by-product.

The objective of this study was to evaluate the potential application of the ice fraction obtained from block freeze concentration of *pinhão* failure extract as a functional component in starch/CMC biodegradable films. Particular emphasis was placed on assessing whether this underexplored fraction could contribute to the development of active, biodegradable packaging materials while simultaneously promoting the full valorization of residues generated during both *pinhão* processing and freeze concentration. The effects of incorporating this fraction on the physicochemical, structural, mechanical, antioxidant, optical, and biodegradation properties of the films were investigated to develop sustainable materials and promote the valorization of an underutilized agro-industrial by-product.

MATERIALS AND METHODS

For block freeze concentration, *Pinhão* failure (*Araucaria angustifolia*), with a particle size ranging from approximately 16 to 30 mesh, was obtained from the Non-Timber Forest Products Technology Laboratory at Embrapa Florestas (25°17′30″ S latitude and 49°13′27″ W longitude). The film-forming solution was prepared using distilled water, corn starch (2000 cps viscosity; Milhena), glycerol (Neon) as a plasticizer, and carboxymethylcellulose (CMC) (food-grade off-white powder; viscosity between 50 and 200 cps; Neon).

Block freeze-concentration

The *Pinhão* failure extract was obtained according to the methodology established by Carvalho et al., with some modifications. The aqueous extract was prepared at a 1:10 (ground *Pinhão* failure/distilled water) ratio in a thermostatic water bath (Tecnal, model TE-184) at 70 °C for 180 minutes with constant mechanical stirring. Subsequently, the solids were removed using a voile strainer (Figure 1a).

Initially, the *Pinhão* failure extract was transferred to 200 mL plastic containers and frozen at –20 ± 2 °C. After freezing, approximately 50% of the original frozen volume was recovered as the liquid fraction upon melting, corresponding to the first concentrate (C1). At the same time, the remaining solid phase was identified as the first ice fraction (I1) (Figure 1b). The liquid fraction obtained in the first stage (C1) was then used as the feed for the second BFC cycle, yielding the second concentrate (C2) and the second ice fraction (I2) (Figure 1b). Thereafter, the concentrate produced during the second stage (C2) underwent a third freeze-concentration step, yielding the third concentrate (C3) and the third ice fraction (I3) (Figure 1b) (Canella et al., 2018).

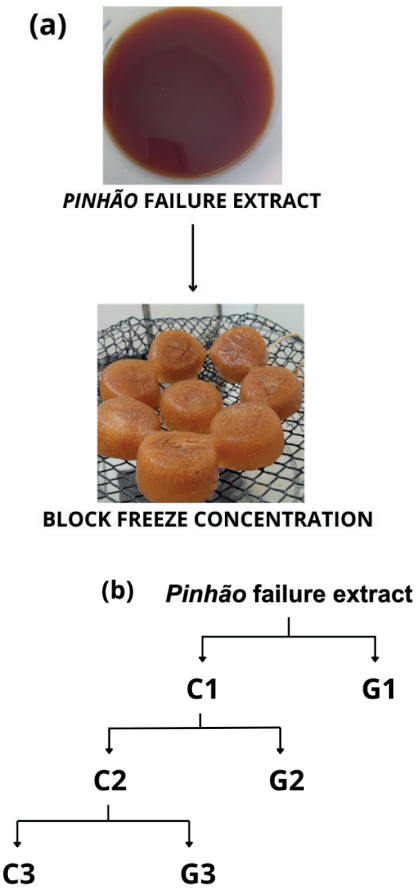

Figure 1. (a) *Pinhão* failure extract, and gravitational-assisted block freeze concentration; (b) Schematic representation of the freeze concentration process applied to *Pinhão* failure extract. C1, C2, and C3 correspond to the concentrates obtained in stages 1, 2, and 3, respectively, while I1, I2, and I3 represent the ice fractions generated during each respective stage.

Block freeze-concentration process parameters

The performance of the freeze concentration process was evaluated by determining the concentration factor (CF) (Aider & Ounis, 2012), with minor adaptations, according to Equation (1):

$$Concentration\ \ Factor = \frac{AG_n}{AG_0} \quad (1)$$

AG_n denotes the gallic acid concentration (mg 100 mL^{-1}) in the concentrated Pinhão failure extract after each freeze-concentration stage, whereas AG_0 represents the gallic acid concentration (mg 100 mL^{-1}) in the initial extract prior to concentration.

Process efficiency (PE) was calculated based on the distribution of gallic acid between the concentrated and ice fractions obtained at the end of each freeze-concentration stage, according to Equation (2):

$$Processes\ \ Efficiency\ (\%) = \frac{AG_C - AG_I}{AG_C} * 100 \quad (2)$$

AGc represents the gallic acid concentration (mg 100 mL^{-1}) in the concentrated fraction, while AGi represents the gallic acid concentration (mg 100 mL^{-1}) in the ice fraction after each concentration cycle.

The ice impurity index was determined from the gallic acid concentration retained in the ice fraction, representing the amount of concentrated solutes entrapped within the frozen matrix. This parameter was expressed as the ratio of the gallic acid concentration in the ice fraction to that observed in the concentrated extract at the end of each freeze-concentration stage. The impurity index for each cycle was calculated using Equation (3):

$$Impurity\ \ of\ \ ice\ (\%) = 100\ (\%) - Processes\ \ Efficiency\ (\%) \quad (3)$$

Film-forming solution preparation

The films were produced using the casting technique (Carvalho et al., 2026; Usman et al., 2016). Initially, 24 g of corn starch was dispersed in 400 mL of distilled water under continuous mechanical stirring. Subsequently, glycerol (13.3 g), used as a plasticizing agent, and 2.4 g of carboxymethylcellulose (CMC) were added to the suspension. The mixture was heated to 50 °C and maintained under constant agitation for approximately 15 min to ensure complete homogenization.

Thereafter, the temperature progressively increased to 80 °C and was maintained for 30 min to promote starch gelatinization and the formation of a uniform film-forming dispersion. Subsequently, the system temperature was elevated to 90 °C and maintained for an additional 15 min.

After cooling the film-forming solution to 40 ± 2 °C, two formulations were prepared. For the active film, 150 mL of the melted ice fraction from the second freeze--concentration stage (I2) was incorporated into the dispersion. In parallel, a control film was prepared under the same processing conditions, without the addition of the I2 fraction.

Both formulations (control and I2-containing films) were subsequently poured into glass plates at a density of 0.08 g cm^{-2} and dried in a forced-air circulation oven at 45 ± 2 °C for 24 h.

The control film formulation was designated as C, whereas the film incorporating the ice fraction obtained from the second freeze-concentration stage (I2) was designated as FI2.

Physical properties

To investigate the physical properties of the developed materials, the films (C and FI2) were characterized for thickness, moisture content, water vapor permeability (WVP), and contact angle.

Film thickness was determined using 5 cm × 5 cm specimens, with measurements taken at five points with a digital micrometer (model 02.0005, ZAAS). Moisture content was quantified by drying samples with previously determined mass in a forced-air oven (Fanem Ltda.) at 105 °C until a constant weight was reached (Carvalho, Hoffmann, et al., 2025; Mueller et al., 2025).

The water vapor permeability (WVP) of the films was determined using a methodology adapted from Hoffmann et al. Water vapor permeability (WVP) was determined by placing 40 g of anhydrous silica gel in 50 mL centrifuge tubes, which were then hermetically sealed with the respective film samples. The sealed systems were stored in a desiccator at 25 °C containing distilled water to maintain 100% relative humidity. The tubes were weighed every 30 min for a total of 4 h. The increase in mass over time was recorded, and the water vapor transmission rate (ΔW/Δt) was obtained from the slope of the linear regression of mass gain versus time. The WVP values were calculated according to Equation 4, in which ΔW/Δt is the slope of the mass gain curve, δ is the film thickness (m), A is the exposed permeation area (m^2), and ΔP is the water vapor pressure difference between the two sides of the film and pure water at 25 °C (Pa).

$$WVP = \left(\frac{\Delta W}{\Delta t}\right) * \frac{\delta}{A * \Delta P} \quad (4)$$

Contact angle measurements were performed based on the method proposed by Jorge et al., with slight modifications. Images were obtained using a USB digital microscope with a magnification capability of up to 1000×. For the analysis, a 10 µL droplet of distilled water was placed onto the film surface, and images of the liquid-surface interaction were recorded immediately after deposition (0 s) and after 180 s. The contact angle values were subsequently determined using ImageJ software.

Mechanical properties

The mechanical behavior of the films was characterized using a universal testing machine (INSTRON EMIC 23-100) in accordance with the ASTM D882 standard method (ASTM D882, 2018). The maximum rupture force and tensile strength were determined using Bluehill Universal software.

Film samples were fixed between two pneumatic grips (EMIC, model GR052; maximum load capacity of 5 kN) and subjected to tensile assays at a constant deformation rate of 1.0 mm s^{-1}.

Tensile strength (TS), elongation at break (EB), and Young's modulus (E) were determined according to Equations (5), (6), and (7), respectively.

$$TS\ [MPa] = \frac{F}{\delta * L} \quad (5)$$

$$EB\ [\%] = \frac{\Delta L}{L_0} \times 100 \quad (6)$$

$$E\ [MPa] = \frac{\sigma}{\varepsilon} \quad (7)$$

F corresponds to the maximum rupture force (N); δ represents the mean film thickness (mm); L refers to the specimen width (mm); ΔL indicates the elongation at the breaking point (mm); L_0 corresponds to the initial length of the film specimen (mm); σ represents tensile strength (MPa); and ε denotes the strain at break (mm/mm).

Structural properties

The thermal behavior of the films was investigated by thermogravimetric analysis (TGA). The samples were heated from room temperature up to 500 °C at a heating rate of 10 °C min^{-1} under an argon atmosphere with a flow rate of 100 mL min^{-1}. Thermogravimetric (TGA) and derivative thermogravimetric (DTG) curves were generated and subsequently analyzed using Origin 8.5 software (Mueller et al., 2025).

Fourier-transform infrared spectroscopy (FTIR) analyses were carried out using a Vertex 70 spectrometer (Bruker, Germany) coupled with an attenuated total reflectance (ATR) accessory. Spectra were collected over the range 400–4500 cm^{-1} at a resolution of 4 cm^{-1}, with 16 scans per sample. The obtained spectra were processed using OPUS software (Bruker) to qualitatively characterize the functional groups present in the films (Carvalho et al., 2026).

The morphological characteristics of the films, including surface topology and cross-sectional structure, were evaluated by scanning electron microscopy (SEM) using a VEGA 3 microscope (Tescan). Before analysis, the samples were coated with a thin gold layer employing a Q150R ES sputter coater (Quorum). Micrographs were obtained under an accelerating voltage of 10 kV. Surface images were recorded at magnifications of 200×, 500×, and 1000×, whereas cross-sectional images were acquired at 400× magnification (Hoffmann et al., 2022).

Colorimetric properties and pH-responsive freshness indicator

Color parameters were determined using a sphere spectrophotometer (SP60, Lovibond) (Carvalho et al., 2026). Color measurements were performed according to the CIELAB color system, in which L* represents lightness, varying from black (0) to white (100); a* indicates the color variation between green (negative values) and red (positive values); and b* corresponds to the chromatic scale ranging from blue (negative values) to yellow (positive values).

The FI2 formulation was evaluated for its pH-responsive freshness-indicator properties. The films were immersed in buffer solutions at pH 4, 7, 10, and 12 to investigate their intelligent response through visually perceptible color variations. Colorimetric parameters (L*, a*, and b*) were determined using a sphere spectrophotometer (SP60, Lovibond). The total color difference (ΔE) was calculated according to Equation (9), where L_0, a_0, and b^*_0 represent the initial color coordinates of the films before exposure to the different pH conditions (Mueller et al., 2024).

Soil burial degradation test

The biodegradation behavior of the films was evaluated by burying the samples in vegetable compost soil under natural environmental conditions. Circular specimens with a diameter of 10 cm were used for the assay. The degradation study was carried out over 42 days, and the biodegradation process was qualitatively monitored via pho-

tographic records. Additionally, the loss of sample mass was periodically determined throughout the experimental period (Carvalho et al., 2026).

Determination of total phenolic content and antioxidant activity

The antioxidant potential of the films (C and FI2) was evaluated by determining total phenolic content and assessing radical-scavenging activity against DPPH and ABTS radicals.

Total phenolic content was quantified using the Folin-Ciocalteu colorimetric method, employing gallic acid as the analytical standard (Singleton & Rossi, 1965). A calibration curve was prepared using gallic acid solutions at concentrations ranging from 1.0 to 9.0 mg L^{-1}, presenting satisfactory linearity (R^2 = 0.99). Aliquots of the sample extracts (0.1- 1.0 mL) were transferred into test tubes, followed by the addition of 1.25 mL of Folin-Ciocalteu reagent and 5 mL of sodium carbonate solution (15%, w/v). After the reaction period, absorbance values were measured at 720 nm using a UV–Vis spectrophotometer (Shimadzu UV-1800, Kyoto, Japan). The results were expressed as milligrams of gallic acid equivalents per gram of film (mg GAE g^{-1}).

The scavenging activity against the DPPH radical was determined by monitoring the reduction of 2,2-diphenyl-1-picrylhydrazyl in the presence of antioxidant compounds contained in the samples. The decrease in absorbance was measured at 517 nm. Antioxidant activity was quantified using a Trolox standard curve, and the results were expressed as micromoles of Trolox equivalents per gram of film (µmol TE g^{-1}) (Brand-Williams et al., 1995).

The ABTS radical cation scavenging capacity was evaluated by assessing the ability of antioxidant compounds to donate hydrogen atoms or electrons to neutralize the $ABTS^{+}$ radical (Re et al., 1999). Absorbance readings were obtained at 734 nm, and antioxidant activity was calculated using Trolox as the reference compound. The results were expressed as µmol TE g^{-1} of film.

Statistical analysis

Statistical analyses were performed using Statistica software (version 13.5, TIBCO). All determinations were carried out in triplicate, and the results were expressed as mean values ± standard deviation. Differences between treatments were assessed by one-way analysis of variance (ANOVA). When statistically significant differences were detected, Tukey's post hoc test was used to compare means. Statistical significance was established at $p < 0.05$ (Prestes, Marafon, et al., 2024).

RESULTS AND DISCUSSION

Block freeze-concentration parameters

Throughout the block freeze-concentration process, the concentration factor increased progressively as the concentration stages advanced, with values of 9.90, 22.13, and 22.50 for C1, C2, and C3, respectively. This behavior demonstrates the gradual enrichment of gallic acid in the concentrated fractions (Table 1). Furthermore, the second concentration stage exhibited the highest process efficiency (53.54 ± 0.10), indicating greater separation efficiency than the other stages and highlighting this step as the most effective phase of the freeze concentration process.

The higher efficiency observed in the second stage may be attributed to more effective separation of ice crystals from the concentrated liquid fraction. In the first stage, part of the gallic acid may remain retained in the ice due to the high water content of the extract. In contrast, during the third stage, the increase in solute concentration likely increased the viscosity of the concentrated fraction, reducing the efficiency of mass and heat transfer within the system (Aider & Ounis, 2012). As a consequence, the formation of purer ice crystals becomes more difficult, favoring the entrapment of solutes in the ice fraction and decreasing the overall efficiency of the freezing concentration process. Therefore, the second stage likely provided the most favorable conditions for gallic acid concentration while minimizing solute retention in the ice phase (Aider & Ounis, 2012; Prestes, Andrade, et al., 2024).

In studies, the performance of acerola pulp (*Malpighia emarginata* DC) during block freeze concentration was evaluated, with emphasis on the retention and concentration of bioactive compounds throughout the process. The concentrate obtained in the third freeze concentration stage showed the greatest enrichment, yielding the highest concentration factor compared with the preceding stages, with values of 127 for C1, 181 for C2, and 270 for C3 (Marafon et al., 2024).

A similar behavior was reported for cold-pressed guabiroba juice subjected to block-freeze concentration, in which the concentration factor increased from 1.6 in the first stage to 2.1 in the second stage, demonstrating progressive enrichment of soluble solids and bioactive compounds throughout the concentration process (Prestes, Andrade, et al., 2024; Prestes, Marafon, et al., 2024).

A comparable trend was observed during the block freeze concentration of yerba mate extract, where the concentration factor progressively increased throughout the process, reaching its highest value in the third stage. The reported CF values were 1.26, 2.08, and 3.05 for stages 1, 2, and 3, respectively, demonstrating the gradual accumulation of gallic acid in the concentrated fractions (Carvalho et al., 2026).

The use of the ice fraction obtained from the second freeze concentration stage (I2) represents a promising strategy for the valorization of process by-products. The C2 concentrate was selected for preliminary application tests, which indicated promising performance (data not shown). Although some bioactive compounds were retained in the ice fraction, as evidenced by an ice retention value of 46.46%, this fraction still contained compounds of technological and functional interest, enabling its subsequent application in the development of active films (Prestes, Marafon, et al., 2024).

The second freeze concentration stage achieved the highest process efficiency, indicating a more favorable balance between solute concentration and separation efficiency. In addition, limiting the process to two stages may offer an important economic advantage, since additional freeze concentration stages generally require higher energy consumption and longer processing times, without necessarily yielding proportional gains in process performance (Boaventura et al., 2013; Prestes, Marafon, et al., 2024).

From a sustainability perspective, reusing the I2 fraction helps reduce process waste and promotes the valorization of materials commonly classified as secondary fractions. Incorporating this fraction into the FI2 film formulation demonstrates its

Stage	Sample	Gallic Acid (mg L^{-1})	CF	EP (%)	Impurity of the Ice (%)
0	*Pinhão* failure extract	1.06 ^{dD} ± 0.01	-	-	-
1	C1	10.5 ^{c} ± 0.01	9.90 ^{c} **± 0.01**	12.57 ^{c} **± 0.20**	-
	I1	9.18 ^{C} ± 0.01	-	-	87.43 ^{a} **± 0.01**
2	C2	23.46 ^{b} ± 0.01	22.13 ^{b} **± 0.01**	53.54 ^{a} ± 0.10	-
	I2	10.9 ^{B} ± 0.01	-	-	46.46 ^{c} ± 0.01
3	C3	23.85 ^{a} **± 0.01**	22.5 ^{a} ± 0.01	46.88 ^{b} **± 0.20**	-
	I3	12.67 ^{A} ± 0.01	-	-	53.12 ^{b} ± 0.01

Table 1. Process efficiency and concentration factor of block freeze concentration of *Pinhão* failure

Results are expressed as the mean ± standard. $^{a, b, c, d}$ Within a column, different superscript lowercase letters denote significant differences ($p < 0.05$) between the *Pinhão* failure extract and C1, C2, and C3. $^{A, B, C, D}$ Within a column, different superscript uppercase letters denote significant differences ($p < 0.05$) between the *Pinhão* failure extract and the I1, I2, and I3 fractions.

Physical properties	C	FI2
Thickness (mm)	0.32 ^{a} **±** 0.05	0.22 ^{b} **±** 0.05
Moisture content (%)	36.17 ^{a} **±** 0.01	27.03 ^{b} **±** 0.01
Water vapor permeability (g $H_2O \cdot m^{-1} \cdot s^{-1} \cdot Pa^{-1}$)	(4.90 ^{b} ± 0.01) × 10^{-8}	(5.80 ^{a} ± 0.01) × 10^{-7}

Table 2. Physical properties of the control sample (C) and film containing ice fraction 2 (FI2)

Results are expressed as the mean ± standard. $^{a, b}$ Within a line, different lowercase superscript letters denote significant differences ($p < 0.05$) between the control sample and the film with the ice fraction from the freeze concentration process of *Pinhão* failure extract.

potential as a functional ingredient for producing high-value, biodegradable materials, thereby aligning with sustainable processing approaches (Carvalho, Ghosh, et al., 2025).

Physical properties

The addition of the I2 fraction reduced film thickness, with FI2 at 0.22 mm and C at 0.32 mm (Table 2). This result may reflect the increased fluidity of the film-forming solution after incorporating I2, allowing the dispersion to spread more easily during casting. As a result, a thinner, more uniformly distributed film layer formed after drying. A similar outcome was reported by de Oliveira et al. observed a reduction in the thickness of rice starch/nanocellulose films after incorporating Amaranthus viridis extract, from 80 to 50 µm, which was associated with the formation of a more compact structure. Likewise, incorporating aqueous fruit extracts into starch-based films can modify the rheological behavior of film-forming dispersions, promoting greater spreading during casting and resulting in thinner film structures (Kupervaser et al., 2023).

A lower moisture content was observed in the FI2 film than in the C (Table 2). This reduction may be associated with interactions between compounds in the I2 fraction and the polymeric matrix, which likely reduced the availability of hydrophilic sites that retain water molecules within the film. In addition, the incorporation of soluble compounds may have promoted a more compact matrix organization, thereby

limiting water retention. Similar behavior was reported by de Oliveira et al. observed a decrease in moisture content after incorporating plant extracts into starch-based films, attributing this effect to structural rearrangements within the polymeric network. Studies also demonstrated that the moisture content of starch films is strongly influenced by structural organization and intermolecular interactions within the matrix, thereby directly affecting water retention capacity (Suh et al., 2020).

It was observed that the films exhibited increased water vapor permeability (WVP), with FI2 showing a value significantly higher than that of the control film. This behavior may be associated with the incorporation of hydrophilic soluble compounds from the I2 fraction into the polymeric matrix, which may have increased the affinity of the film for water molecules and favored water vapor transport. Although SEM images indicated that FI2 maintained a continuous and compact surface morphology, the presence of polar compounds within the matrix may have increased molecular mobility and created preferential pathways for water vapor diffusion. Therefore, the higher WVP observed for FI2 appears to be more related to changes in the chemical affinity of the matrix for water than to the formation of visible structural defects. The incorporation of natural additives into starch films can increase water vapor permeability because of modifications in matrix organization and increased hydrophilicity of the system (Singh et al., 2024).

The FI2 film exhibited higher water contact angles than the control sample (C) at both evaluation times, indicating reduced surface wettability after incorporation of the I2 fraction (Table 3). At 0 s, the contact angles of FI2 were 59.4° and 62.6°, whereas the control film showed 33.7° and 35.6 °, respectively. After 180 s, FI2 maintained higher contact angles (55.1° and 59.5°) than C (28.3° and 35.3°).

The reduction in contact angle over time indicates greater spreading of the water droplet and/or progressive penetration of water into the polymeric matrix, which is characteristic of films rich in hydroxyl groups, such as starch, CMC, and glycerol (Figure 2). These compounds strongly interact with water molecules through hydrogen bonding. In general, contact angle measurements are used to assess a surface's hydrophobicity: higher values indicate greater hydrophobicity, while values below 90° are characteristic of hydrophilic materials. In the present study, all films exhibited contact angles below 90°, confirming the hydrophilic nature of the polymeric matrix and its affinity for water, consistent with the reduction in contact angle observed between 0 and 180 s (Regmi & Janaswamy, 2024).

However, the smaller reduction observed for FI2 suggests that incorporating the I2 fraction reduced the interaction between the film surface and water molecules. This behavior may be associated with structural modifications induced by compounds present in the I2 fraction, which may have reduced the exposure of hydrophilic groups on the film surface and promoted a more organized polymeric network. A similar tendency was observed in starch-based intelligent films incorporating natural residues, in which the addition of bioactive compounds altered surface interactions and wettability by modifying the structural organization of the polymeric matrix (Ramírez et al., 2012).

Water contact angles	Time			
	0 s		180 s	
Sample	Left angle	Right angle	Left angle	Right angle
C (°)	33.7 [b] ± 0.01	35.6 [b] ± 0.01	28.3 [b] ± 0.01	35.3 [b] ± 0.01
FI2 (°)	59.4 [a] ± 0.01	62.6 [a] ± 0.01	55.1 [a] ± 0.01	59.5 [a] ± 0.01

Table 3. Water contact angles of the control sample (C) and film containing ice fraction 2 (FI2)

Results are expressed as the mean ± standard. [a, b] Within a column, different lowercase superscript letters denote significant differences ($p < 0.05$) between the control sample and the film with the ice fraction from the freeze-concentration process of *Pinhão* failure extract.

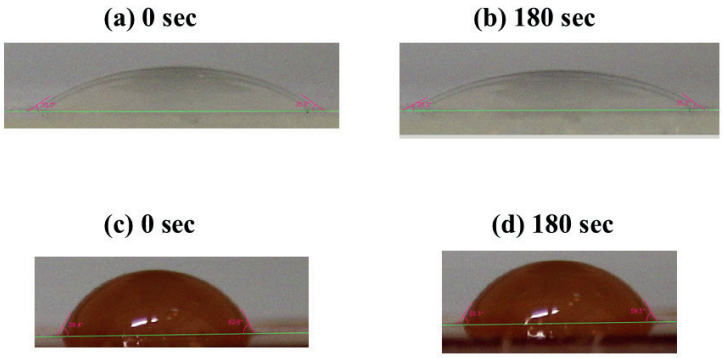

Figure 2. Water contact angle measurements of the films at different evaluation times: (a) control film (C) at 0 s; (b) control film (C) at 180 s; (c) FI2 film at 0 s; and (d) FI2 film at 180 s.

Mechanical properties	C	FI2
Tensile strength (MPa)	1.64 [b] ± 0.01	2.65 [a] ± 0.01
Elongation at break (%)	37.50 [b] ± 0.01	57.65 [a] ± 0.01
Young's Modulus (MPa)	3.81 [a] ± 0.01	4.00 [a] ± 0.01

Table 4. Mechanical properties of the control sample (C) and film containing ice fraction 2 (FI2)

Results are expressed as the mean ± standard. [a, b] Within a line, different lowercase superscript letters denote significant differences ($p < 0.05$) between the control sample and the film with the ice fraction from the freeze-concentration process of Pinhão failure extract.

Mechanical properties

The incorporation of the I2 fraction improved the mechanical performance of the films, particularly tensile strength and elongation at break (Table 4). FI2 showed higher tensile strength (2.65 MPa) than the control film (1.64 MPa), indicating greater resistance to rupture. In addition, elongation at break increased from 37.50% in C to 57.65% in FI2, suggesting that incorporating I2 increased film flexibility and allowed greater deformation before rupture. However, Young's modulus did not differ significantly between the formulations, indicating that the stiffness of the polymeric matrix was not substantially affected by the addition of I2. FI2 exhibited improved resistance and flexibility while maintaining a rigidity similar to that of the control film.

Similar behavior was reported by Chavez-Marquez et al. observed that incorporating anthocyanins and molle essential oil into potato starch films increased tensile strength and elongation at break, attributed to improved compatibility and intermolecular interactions within the polymeric network. Priyadarshi & Rhim demonstrated that incorporating bioactive compounds into biodegradable starch films can enhance mechanical resistance and flexibility by promoting stronger interactions between polymer chains, without significantly altering film rigidity. These findings support the results obtained for FI2, suggesting that the compounds present in the I2 fraction contributed to the reinforcement and stabilization of the polymeric matrix.

Structural properties

The TGA/DTG curves showed distinct thermal behaviors between the control film and FI2. The control film exhibited higher thermal stability, with the main thermal degradation event starting at approximately 410 °C and ending near 510 °C (Figure 3a,b). This event was also confirmed by the DTG curve, which showed an intense and well-defined mass loss peak around 480-490 °C, indicating the major decomposition of the starch/CMC/glycerol polymeric matrix.

The lower degradation temperature observed for FI2 may be related to the presence of low-molecular-weight compounds and soluble constituents retained in the I2 fraction, which are generally more thermolabile than the polysaccharide matrix (Figure 3c,d). Similar behavior has been reported in starch-based films containing natural extracts or bioactive additives, where incorporating these compounds altered the thermal degradation profile due to changes in polymer–additive interactions and the presence of components with different thermal resistances. Studies have reported that incorporating bioactive compounds into biodegradable films can modify the thermal behavior of the polymeric matrix, depending on the compatibility and interactions between the added compounds and the biopolymer network (Priyadarshi & Rhim, 2020). Santhosh et al. also emphasized that thermal stability in starch-based films is strongly influenced by the polymer source, plasticizer, and incorporated bioactive compounds.

The DTG curve of the control film showed a more intense and well-defined peak, suggesting a more uniform degradation process of the base matrix. Conversely, FI2 exhibited a broader degradation profile at lower temperatures, suggesting a more complex thermal decomposition process, likely due to the simultaneous degradation of starch/CMC/glycerol and compounds introduced by the I2 fraction. Similar behavior was described by Charles et al. in chitosan-starch films containing natural extracts, where the addition of plant extracts altered the films' thermal degradation pattern due to interactions between the polymeric matrix and the extract components.

Although FI2 showed lower thermal stability than the control film, its primary degradation event occurred above 200 °C, a temperature typically encountered during storage and in most food packaging applications. Therefore, incorporating I2 modified the thermal degradation profile but did not necessarily compromise the material's applicability as a biodegradable food packaging film.

(a)

TGA Controle

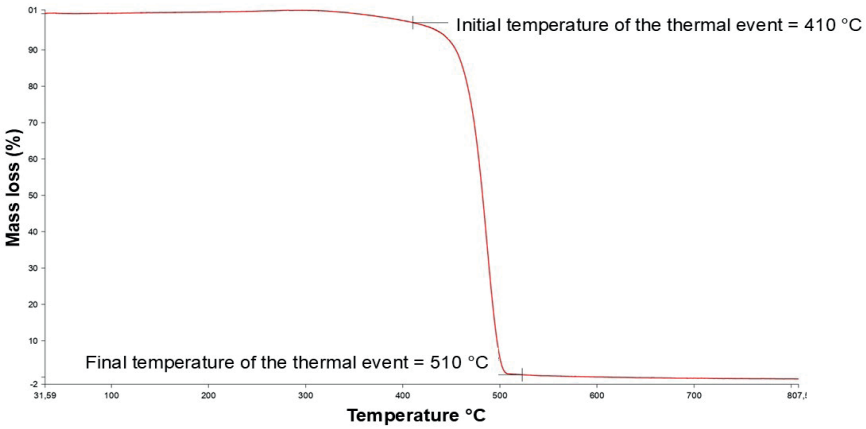

(b)

DTG Controle

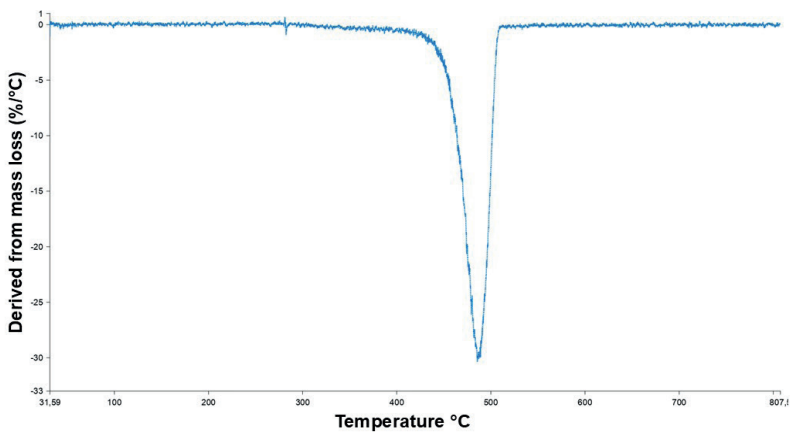

(c)

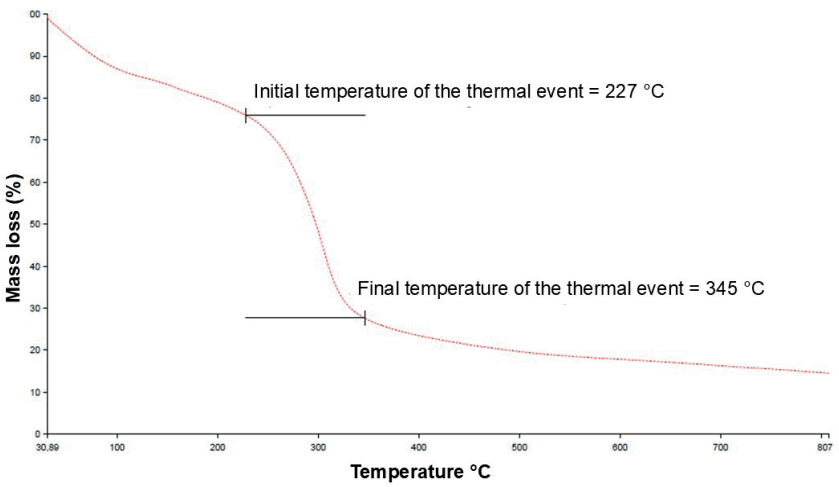

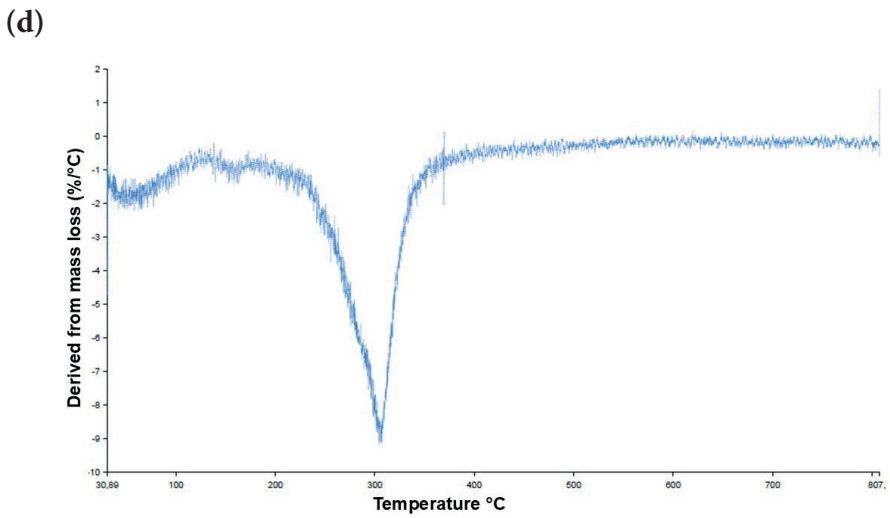

Figure 3. Thermogravimetric (TGA) and derivative thermogravimetric (DTG) curves of the analyzed films: (a) TGA curve of the control film (C); (b) DTG curve of the control film (C); (c) TGA curve of the FI2 film; and (d) DTG curve of the FI2 film.

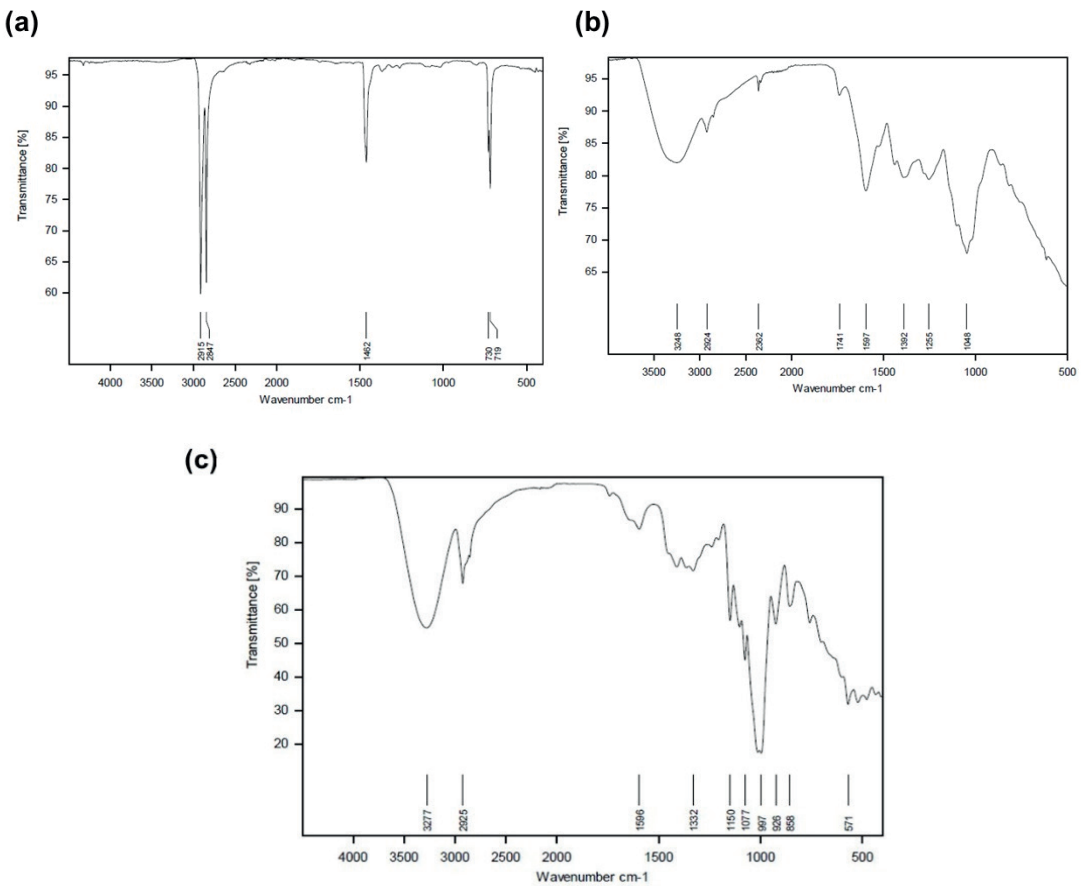

Figure 4. FTIR spectra of the analyzed samples: (A) control film; (B) pinhão failure ice fraction from the second freeze concentration stage (I2); and (C) FI2 film sample.

The FTIR spectra of the control film (C) and the film containing the ice fraction from the second freeze concentration stage (FI2) exhibited similar absorption profiles, indicating that incorporating the I2 fraction did not substantially alter the chemical structure of the polymeric matrix. Both films exhibited a broad absorption band at approximately 3276-3277 cm^{-1}, attributed to O-H stretching vibrations of starch, carboxymethylcellulose, glycerol, and adsorbed water molecules (Figure 4a,c). The bands observed near 2925-2926 cm^{-1} correspond to C-H stretching vibrations of aliphatic groups, while the absorptions located around 1150-1151 and 1076-1077 cm^{-1} are characteristic of C-O and C-O-C stretching vibrations typically found in polysaccharide-based materials. Furthermore, the bands identified near 1596 cm^{-1} and 1331-1332 cm^{-1} are associated with carboxylate groups and molecular interactions commonly observed in starch–CMC matrices (Kizil et al., 2002).

The spectrum of the I2 fraction showed characteristic bands at 3248, 1741, 1597, 1392, 1255, and 1048 cm^{-1} (Figure 4b), indicating the presence of hydroxyl-, carbonyl-, and ether-containing compounds retained during the freeze-concentration process (Kizil et al., 2002). Although these bands were not clearly observed in the FI2 spectrum, likely due to overlap with the intense signals from starch and CMC, slight shifts were detected in the fingerprint region after incorporation of the I2 fraction. In particular, the bands located at 999 and 924 cm^{-1} in the control film shifted to 997 and 926 cm^{-1}, respectively, in FI2. Similar shifts have been reported in starch-based films containing natural additives and are generally associated with intermolecular interactions between the incorporated compounds and the polymeric matrix (Pelissari et al., 2014; Sapper et al., 2019).

The absence of new absorption bands indicates that incorporating the I2 fraction did not induce significant chemical modifications in the film structure. Similar behavior has been reported for starch-based films containing natural additives, where the absence of new bands, combined with slight shifts in characteristic absorption regions, was attributed to intermolecular interactions, particularly hydrogen bonding, rather than to the formation of new covalent bonds (Pelissari et al., 2014; Sapper et al., 2019). According to these authors, interactions between hydroxyl-rich compounds and polysaccharide chains can alter the organization of the polymeric network while preserving its original chemical identity.

These findings are consistent with the physicochemical, mechanical, and morphological properties observed for FI2. The intermolecular interactions suggested by the FTIR results may have contributed to the lower moisture content, higher tensile strength, and more compact morphology observed by SEM. Similar relationships between enhanced intermolecular interactions and improvements in film cohesion, barrier properties, and structural stability have been reported in starch-based biodegradable films containing plant-derived compounds (Pelissari et al., 2014; Sapper et al., 2019). Therefore, the FTIR results indicate that the I2 fraction served as a functional additive, modifying the structural organization of the starch-CMC matrix without altering its fundamental chemical structure.

Scanning electron microscopy (SEM) micrographs are presented in Figure 5. Both samples exhibited continuous, homogeneous surfaces with no evident structural defects. The control film (Figure 5a) showed a relatively uniform matrix at both 200×

and 1000× magnifications, with small irregularities distributed across the surface, features commonly reported in biodegradable films (Carvalho et al., 2026; Gómez-Bachar et al., 2024; Sanchez et al., 2024).

The incorporation of the ice fraction did not significantly alter the material's surface morphology. SEM images of the FI2 film (Figure 5b) revealed a similarly continuous and compact surface. The absence of pores or visible discontinuities suggests that the compounds derived from the ice fraction were adequately dispersed within the polymeric matrix during film formation. The most evident differences between the samples were observed in the cross-sectional morphology. While the control film exhibited a relatively uniform internal structure throughout its thickness, FI2 showed a more heterogeneous cross-sectional organization. This behavior may be associated with the incorporation of compounds present in the ice fraction, such as soluble solids and other low-molecular-weight constituents, which may have influenced the arrangement of the starch-CMC network during film formation and drying. Despite the greater heterogeneity observed in the cross-section, no cracks, pores, phase separation, or structural discontinuities were detected, indicating good compatibility between the incorporated compounds and the polymeric matrix. Therefore, the incorporation of I2 modified the internal organization of the film while preserving the structural integrity and continuity of the material (Gómez-Bachar et al., 2024; Sirbu et al., 2024).

Similar results have been reported for biodegradable films containing plant extracts and other sources of bioactive compounds, in which incorporating these components promotes changes in microstructural organization and increases cross-sectional roughness. These modifications are generally attributed to the interactions established between the incorporated compounds and the polymer chains, which influence molecular packing and the structural organization of the matrix during film formation (Carvalho et al., 2026; Gómez-Bachar et al., 2024; Sanchez et al., 2024; Sirbu et al., 2024).

Colorimetric properties and pH-responsive freshness indicator

The incorporation of the ice fraction obtained from freeze concentration significantly affected the optical properties of the films (Table 5 and Figure 6). The control film (C) exhibited high lightness (L* = 88.44) and low a* (1.19) and b* (2.70) values, resulting in a translucent, slightly yellowish appearance. In contrast, the film containing the ice fraction (FI2) showed a significant decrease in lightness (L* = 68.73) and a marked increase in both a* (24.13) and b* (44.54), resulting in a more intense orange coloration (Figure 6a).

These changes can be attributed to the incorporation of compounds present in the ice fraction, including phenolic compounds and natural pigments retained during the freeze concentration process (Prestes et al., 2022; Silveira Hornung et al., 2020). The presence of these compounds increases light absorption in the visible region of the spectrum, reducing film transparency and enhancing color intensity. Similar results have been reported for biodegradable films incorporating plant extracts rich in bioactive compounds, in which the addition of phenolic compounds led to decreased lightness and increased color saturation (Carvalho et al., 2026; Priyadarshi & Rhim, 2020; J. Zhang et al., 2024).

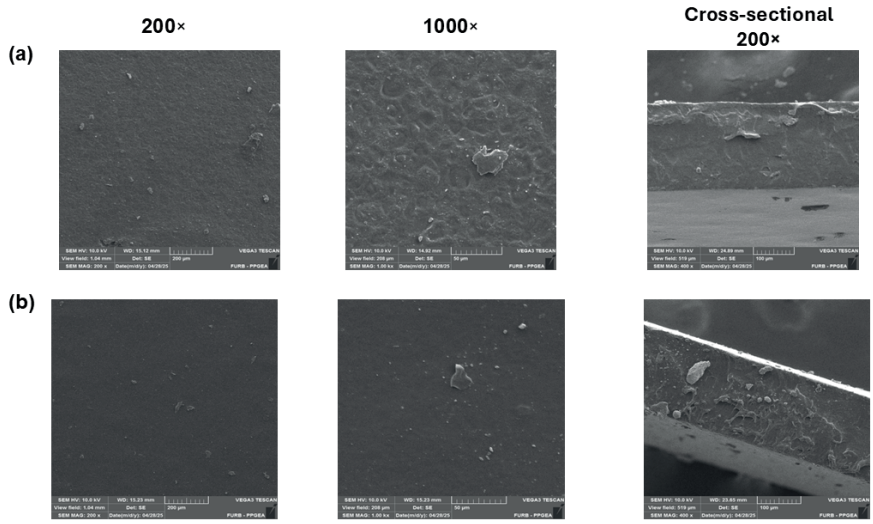

Figure 5. Scanning electron microscopy (SEM) micrographs of the films: (a) control film surface at 200× and 1000× magnification, and cross-sectional morphology at 400×; (b) FI2 film surface at 200× and 1000× magnification, and cross-sectional morphology at 400×.

Sample	L*	a*	b*	ΔE
C	88.44 ^{a} ± 0.35	1.19 ^{f} ± 0.03	2.70 ^{f} ± 0.15	-
FI2	68.73 ^{b} ± 1.86	24.13 ^{a} ± 1.45	44.54 ^{d} ± 1.89	-
FI2 – pH 4	64.53 ^{c} ± 2.58	9.06 ^{e} ± 1.05	47.62 ^{c} ± 2.51	15.94 ^{c} ± 1.00
FI2 – pH 7	58.97 ^{d} ± 3.62	13.47 ^{d} ± 1.60	43.63 ^{e} ± 2.96	14.48 ^{c} ± 1.24
FI2 – pH 10	49.62 ^{e} ± 3.89	19.64 ^{c} ± 2.01	50.23 ^{a} ± 3.07	20.44 ^{b} ± 2.10
FI2 – pH 12	43.47 ^{f} ± 4.01	21.42 ^{b} ± 2.00	49.62 ^{b} ± 2.55	25.91 ^{a} ± 2.08

Table 5. Color parameters (CIELAB) and total color difference (Δ*E*) of the control sample (C), film (FI2), and film (FI2) under different pH conditions

Results are expressed as the mean ± standard. $^{a, b, c, d, e, f}$ Within a column, different lowercase superscript letters denote significant differences ($p < 0.05$).

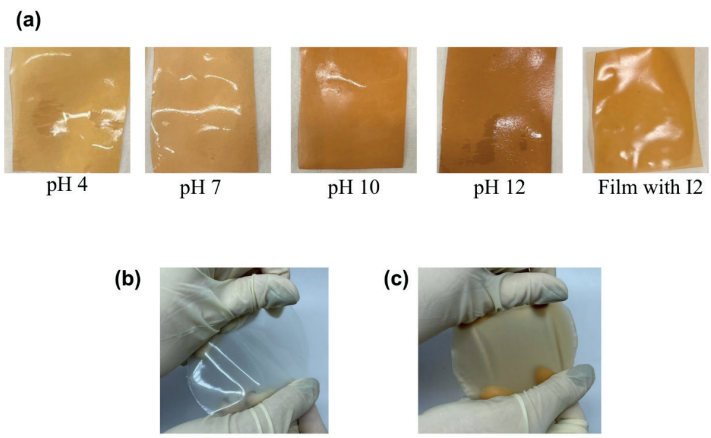

Figure 6. (a) Visual color changes of the FI2 film after exposure to pH 4, 7, 10, and 12 solutions; (b) control film (C); and (c) FI2 film.

In addition to the differences observed between C and FI2, the film containing the ice fraction exhibited a pH-dependent response (Figure 6a). As the pH increased from 4 to 12, lightness decreased significantly, with L* values decreasing from 64.53 to 43.47 ($p < 0.05$). Simultaneously, the a* parameter increased from 9.06 to 21.42, indicating an intensification of reddish tones, while b* values remained high under all evaluated conditions. Together, these changes promoted a gradual shift toward more intense orange hues under alkaline conditions, as visually observed in Figure 6a. The film images (Figure 6b,c) corroborate the colorimetric analysis results, demonstrating that incorporating the ice fraction intensified the matrix coloration compared with the control film. Despite this visual change, the films maintained a homogeneous appearance and continuous surface, with no apparent macroscopic defects, suggesting favorable interactions between the compounds present in the ice fraction and the polymeric matrix (Cui et al., 2021; Dăescu et al., 2024; Suhag et al., 2020).

The observed behavior suggests that the bioactive compounds present in the ice fraction undergo structural modifications in response to pH variations. Phenolic compounds are particularly sensitive to environmental changes and may exhibit altered optical properties due to functional-group ionization, which affects light absorption and, consequently, the perceived color. This effect is generally more pronounced under alkaline conditions, which may explain the greater color intensity observed in films exposed to higher pH values (Carvalho et al., 2026; Carvalho, Hoffmann, et al., 2025; Cheng et al., 2022; Priyadarshi et al., 2021; Z. Zhang et al., 2019).

The total color difference (ΔE) corroborated the results obtained for the colorimetric parameters. Values ranged from 14.48 to 25.91, with the highest values observed at pH 10 and 12. Given that color differences greater than 2 can already be visually perceived (Marafon et al., 2024), all treatments exhibited color changes readily distinguishable to the naked eye. Furthermore, the progressive increase in ΔE under alkaline conditions confirms that the intensity of the chromatic changes was pH-dependent (Benbettaïeb et al., 2019; Cui et al., 2021; Silveira Hornung et al., 2020).

The spoilage of many foods is associated with the formation of alkaline compounds that increase the pH of the surrounding environment. In this context, the observed visual changes, particularly at pH 10 and 12, indicate that the FI2 film has potential as a colorimetric indicator in intelligent packaging systems. Therefore, the incorporation of the ice fraction imparted a pH-dependent visual response to the film, expanding its potential application for food quality monitoring (Benbettaïeb et al., 2019; Sales et al., 2021).

Soil burial degradation test

The soil burial degradation test demonstrated that both films exhibited progressive mass loss throughout the composting period, confirming the biodegradable nature of the starch-based polymeric matrices. However, differences in the degradation profiles were observed between the formulations (Figure 7). The control film was completely degraded after 39 days (Figure 8a), whereas the FI2 film required 42 days for complete degradation (Figure 8b), indicating that incorporating the I2 fraction slightly delayed biodegradation.

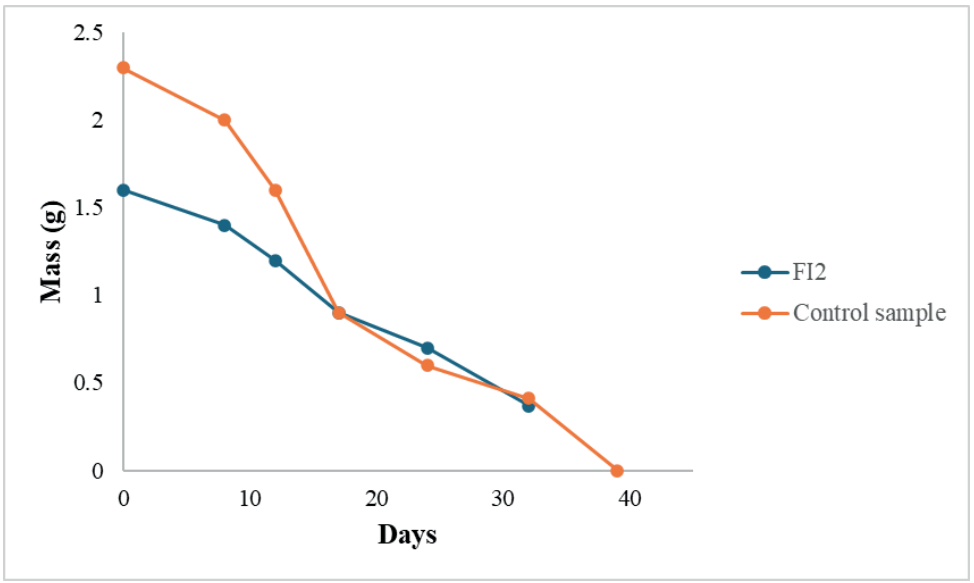

Figure 7. Mass loss profile of the biodegradable films during the soil biodegradation assay. The orange curve corresponds to the control film (C), whereas the blue curve represents the FI2 film. The y-axis indicates mass loss, while the x-axis represents the biodegradation period (days).

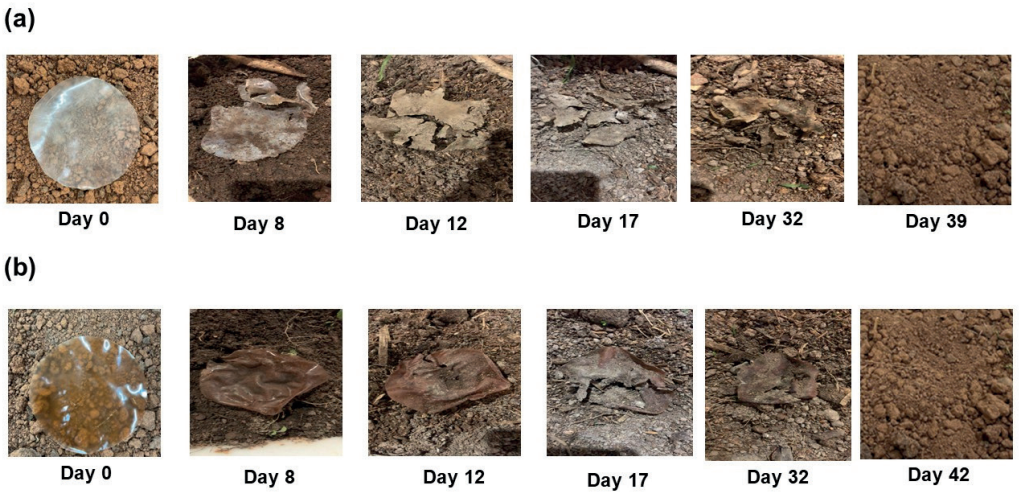

Figure 8. Soil burial degradation behavior of the films during storage in vegetal compost soil: (a) control film (C) at days 0, 8, 12, 17, 32, and 39; and (b) FI2 film at days 0, 8, 12, 17, 32, and 39.

Antioxidant Parameter	C	FI2
Total phenolic content (mg GAE g^{-1})	ND	12.99 ± 1.08
DPPH (μmol TE g^{-1})		1818.20 ± 5.67
ABTS + (μmol TE g^{-1})		3962.20 ± 3.73

Table 6. TPC and antioxidant activity of the control sample (C) and film (FI2).

ND = Not Detected. Results are expressed as the mean ± standard.

The slower degradation of FI2 may be attributed to the structural modifications promoted by the compounds present in the I2 fraction. Compared with the control film, FI2 exhibited lower moisture content (27.03%; control sample: 36.17%) and higher water contact angles, indicating lower water affinity and reduced water uptake capacity. Since water absorption is a critical step in the biodegradation of starch-based materials, lower water uptake can delay swelling, hydrolysis, and microbial colonization of the polymeric matrix. As water penetrates the structure, intermolecular interactions between starch chains become weaker, facilitating enzymatic attack and polymer disintegration (Mali et al., 2006).

This hypothesis is supported by the SEM micrographs (Figure 5), which reveal a more compact and cohesive morphology in FI2 than in the control film. The denser structure likely reduced water diffusion and microbial accessibility within the matrix, contributing to slower degradation kinetics. Moreover, FI2 exhibited higher tensile strength than the control film, suggesting stronger intermolecular interactions within the polymeric network. Similar observations were reported by Othman et al. found that films with more compact morphologies exhibited lower water absorption and delayed degradation during soil burial tests due to reduced permeability and microbial access. Also, Shahrim et al. demonstrated that starch-based films with more organized structures and stronger intermolecular interactions showed slower biodegradation rates under soil conditions.

Despite the slightly slower degradation, FI2 still exhibited complete biodegradation within 42 days. This result demonstrates that incorporating the freeze-concentrated I2 fraction improved the films' structural stability without compromising their environmental degradability. Therefore, FI2 combines enhanced functional properties with rapid biodegradation.

Total phenolic content and antioxidant activity

The incorporation of the ice fraction obtained from the second stage of block freeze concentration (I2) introduced antioxidant compounds into the film matrix (Table 6). While phenolic compounds were not detected in the control film, FI2 presented 12.99 ± 1.08 mg GAE g^{-1}, indicating that part of the bioactive compounds originally present in the pinhão extract remained associated with the ice fraction and were retained after film formation.

Pinhão (*Araucaria angustifolia*) has been described as a source of bioactive compounds with antioxidant potential, including phenolic constituents that act as reducing agents and free-radical scavengers (A. de Oliveira et al., 2021). Although block freeze concentration promotes the preferential migration of solutes to the concentrated fraction, complete separation is not achieved. As shown in Table 1, the I2 fraction contained an ice impurity of 46.46%, indicating that a considerable amount of soluble material remained trapped within the frozen matrix. Similar behavior has been reported during the freeze concentration of acerola pulp, where bioactive compounds were partially retained in the ice phase throughout the process (Marafon et al., 2024). Therefore, the detection of phenolic compounds in FI2 was expected and reflects incomplete solute exclusion during ice crystal formation.

The antioxidant activity measured by DPPH and ABTS followed the same trend observed for total phenolic content. FI2 showed values of 1818.20 ± 5.67 μmol TE g^{-1} and 3962.20 ± 3.73 μmol TE g^{-1} for DPPH and ABTS, respectively. Since phenolic compounds were not detected in the control film, the antioxidant response observed in FI2 was most likely attributable to compounds incorporated via the I2 fraction. Similar observations have been reported for freeze-concentrated plant matrices, in which the preservation of phenolic compounds led to increased antioxidant activity after processing (Boaventura et al., 2013; Marafon et al., 2024).

The higher values obtained by the ABTS assay than by the DPPH assay are consistent with the distinct reaction mechanisms underlying these methods. According to Re et al., the ABTS radical can react with a wider range of antioxidant compounds, including molecules with different polarities, whereas DPPH tends to be more selective. This difference may explain the stronger response observed in the ABTS assay and suggests that the retained compounds in the I2 fraction include molecules capable of acting through multiple antioxidant pathways.

The antioxidant profile of FI2 agrees with other characteristics observed in the film. The lower lightness and higher a* and b* values found in Table 5 indicate the incorporation of colored compounds from the I2 fraction into the polymeric matrix. Likewise, the slight shifts observed in the FTIR spectra after the addition of I2 suggest interactions between these compounds and the starch-CMC network. Although no new functional groups were identified, such interactions may have contributed to the retention of antioxidant compounds within the film's structure throughout drying and storage.

A comparable approach was reported by Carvalho et al. incorporated residual fractions generated during the block freeze concentration of yerba mate extract into biodegradable films. The authors observed that compounds remaining in secondary fractions could provide functional properties to the resulting materials, demonstrating that fractions commonly regarded as process residues can still represent valuable sources of bioactive compounds. Similar conclusions were reported by Prestes, Marafon, et al. showed that ice fractions obtained during the freeze concentration of guabiroba juice retained compounds of functional interest despite their separation from the concentrated phase.

Rather than being discarded, the I2 fraction was successfully converted into a functional component of the film formulation. The antioxidant activity observed in FI2 suggests potential application as an active packaging material, particularly for foods susceptible to oxidative deterioration. These results underscore the potential to valorize freeze-concentration side streams while simultaneously enhancing the functionality of biodegradable packaging systems.

4. CONCLUSION

The results demonstrated that the ice fraction obtained from the second stage of block freeze concentration of *Pinhão* failure extract possesses significant technological potential and should not be regarded merely as a process by-product. The block freeze concentration process effectively concentrated gallic acid, with the second stage presenting the highest process efficiency and providing an ice fraction rich in compounds of technological interest.

The incorporation of the I2 fraction into starch–CMC films improved mechanical performance by increasing tensile strength and elongation at break without affecting film rigidity. In addition, FI2 films exhibited lower moisture content, greater surface hydrophobicity, antioxidant activity, and pH-responsive color changes, indicating their potential application as active and intelligent packaging materials (smart material). FTIR and SEM analyses suggested that the compounds retained in the ice fraction interacted with the polymeric matrix, modifying its structural organization without promoting significant chemical changes.

Although the incorporation of I2 slightly delayed biodegradation, complete degradation was achieved within 42 days, confirming the environmentally friendly nature of the developed materials. Therefore, the valorization of the ice fraction generated during block freeze concentration represents an innovative and sustainable strategy for developing biodegradable packaging materials while promoting the circular use of agro-industrial by-products.

Funding: This research was funded by the National Council for Scientific and Technological Development (CNPq, Brazil) [303069/2022-8; 174429/2023-1; 302867/2023-6], and by a scholarship from the Coordination for the Improvement of Higher Education Personnel (CAPES, Brazil-Finance Code 001). Financial support was also provided by the Foundation for Research Support of the State of Rio de Janeiro (FAPERJ) and the Foundation for Research and Innovation Support of the State of Santa Catarina (FAPESC) (TO2025TR001604), as well as the Ministry of Science, Technology and Innovation (MCTI), Brazil.

Acknowledgments: The authors thank CAPES (Coordination of Improvement of Higher Education Personnel, Brazil-Finance Code 001) and CNPq (National Council for Scientific and Technological Development, Brazil) for the scholarships.

REFERENCES

Aider, M., & Ounis, W. Ben. (2012). Skim milk cryoconcentration as affected by the thawing mode: gravitational vs. microwave-assisted. *International Journal of Food Science & Technology*, *47*(1), 195–202. https://doi.org/10.1111/j.1365-2621.2011.02826.x

Asrafali, S. P., Periyasamy, T., & Lee, J. (2026). Biopolymer-Based Active and Intelligent Food Packaging: Recent Advances in Materials, Technologies, and Applications. *Polymers*, *18*(2), 196. https://doi.org/10.3390/polym18020196

ASTM D882. (2018). *Standard Test Method for Tensile Properties of Thin Plastic Sheeting.*

Beghetto, V., Conca, S., & Santandrea, D. (2026). Carboxymethyl Cellulose-Based Films for Sustainable Food Packaging: Modification Strategies and Structure–Property Relationships. *Polymers*, *18*(5), 552. https://doi.org/10.3390/polym18050552

Benbettaïeb, N., Karbowiak, T., & Debeaufort, F. (2019). Bioactive edible films for food applications:Influence of the bioactive compounds on film structure and properties. *Critical Reviews in Food Science and Nutrition*, *59*(7), 1137–1153. https://doi.org/10.1080/10408398.2017.1393384

Boaventura, B. C. B., Murakami, A. N. N., Prudêncio, E. S., Maraschin, M., Murakami, F. S., Amante, E. R., & Amboni, R. D. de M. C. (2013). Enhancement of bioactive compounds content and antioxidant activity of aqueous extract of mate (Ilex paraguariensis A. St. Hil.) through freeze concentration technology. *Food Research International*, *53*(2), 686–692. https://doi.org/10.1016/j.foodres.2012.07.042

Brand-Williams, W., Cuvelier, M. E., & Berset, C. (1995). Use of a free radical method to evaluate antioxidant activity. *LWT - Food Science and Technology*, *28*(1), 25–30. https://doi.org/10.1016/S0023-6438(95)80008-5

Canella, M. H. M., Munoz, I. de B., Pinto, S. S., de Liz, G. R., Muller, C. M. O., Amboni, R. D. de M. C., & Prudencio, E. S. (2018). Use of Concentrated Whey by Freeze Concentration Process to Obtain a Symbiotic Fermented Lactic Beverage. *Advance Journal of Food Science and Technology*, *14*(2), 56–68. https://doi.org/10.19026/ajfst.14.5832

Carvalho, A. C. F., Ghosh, S., Hoffmann, T. G., Prudêncio, E. S., de Souza, C. K., & Roy, S. (2025). Valuing agro-industrial waste in the development of sustainable food packaging based on the system of a circular bioeconomy: A review. *Cleaner Waste Systems*, *11*, 100275. https://doi.org/10.1016/j.clwas.2025.100275

Carvalho, A. C. F., Hoffmann, T. G., Helm, C. V., Prudêncio, E. S., Roy, S., & de Souza, C. K. (2025). Smart biopolymer based on rice husk extracts and Pinhão failure applied as an interlayer for sliced mozzarella cheese. *Journal of Vinyl and Additive Technology*. https://doi.org/10.1002/vnl.22222

Carvalho, A. C. F., Prebianca, J., Marafon, K., Prestes, A. A., Andrade, D. R. M., Helm, C. V., Gois, J. S. de, Tedeschi, P., de Souza, C. K., & Prudêncio, E. S. (2026). Application of Residues from Block Freeze-Concentrated Yerba Mate (Ilex paraguariensis) Extract as Functional Agents in Smart Biopolymeric Systems Under a Circular Economy Perspective. *Processes*, *14*(7), 1122. https://doi.org/10.3390/pr14071122

Casas-Forero, N., Orellana-Palma, P., & Petzold, G. (2020). Influence of block freeze concentration and evaporation on physicochemical properties, bioactive compounds and antioxidant activity in blueberry juice. *Food Science and Technology*, *40*(suppl 2), 387–394. https://doi.org/10.1590/fst.29819

Cazón, P., Mateus, A. R., & Silva, A. S. (2025). Advances in active packaging using natural biopolymers and fruit by-products for enhanced food preservation. *Food Research International*, *213*, 116439. https://doi.org/10.1016/j.foodres.2025.116439

Charles, A. L., Motsa, N., & Abdillah, A. A. (2022). A Comprehensive Characterization of Biodegradable Edible Films Based on Potato Peel Starch Plasticized with Glycerol. *Polymers*, *14*(17), 3462. https://doi.org/10.3390/polym14173462

Chavez-Marquez, E., Bernedo, M. S. B., de Jara, E. M., Quequezana-Bedregal, M. J., Gutierrez-Oppe, E. E., & Pessôa Filho, P. de A. (2023). Development of intelligent and active potato starch films based on purple corn cob extract and molle essential oil. *International Journal of Biological Macromolecules*, *242*, 125080. https://doi.org/10.1016/J.IJBIOMAC.2023.125080

Cheng, M., Cui, Y., Yan, X., Zhang, R., Wang, J., & Wang, X. (2022). Effect of dual-modified cassava starches on intelligent packaging films containing red cabbage extracts. *Food Hydrocolloids*, *124*, 107225. https://doi.org/10.1016/j.foodhyd.2021.107225

Cui, C., Ji, N., Wang, Y., Xiong, L., & Sun, Q. (2021). Bioactive and intelligent starch-based films: A review. *Trends in Food Science & Technology*, *116*, 854–869. https://doi.org/10.1016/j.tifs.2021.08.024

Dăescu, D. I., Dreavă, D. M., Todea, A., Peter, F., & Păușescu, I. (2024). Intelligent Biopolymer-Based Films: Promising New Solutions for Food Packaging Applications. *Polymers*, *16*(16), 2256. https://doi.org/10.3390/polym16162256

de Oliveira, A., Moreira, T. F. M., Pepinelli, A. L. S., Costa, L. G. M. A., Leal, L. E., da Silva, T. B. V., Gonçalves, O. H., Porto Ineu, R., Dias, M. I., Barros, L., Abreu, R. M. V., Ferreira, I. C. F. R., Bracht, L., & Leimann, F. V. (2021). Bioactivity screening of pinhãoAraucaria Angustifolia (Bertol.) Kuntze) seed extracts: the inhibition of cholinesterases and α-amylases, and cytotoxic and anti-inflammatory activities. *Food & Function*, *12*(20), 9820–9828. https://doi.org/10.1039/D1FO01163D

de Oliveira, J. P., de Souza Moreira, V., de Oliveira, J. S., Landim, L. B., da Silva, N. M. C., & de Oliveira, C. P. (2025). Development and characterization of biodegradable active films based on rice starch with nanocellulose and Amaranthus viridis extract. *International Journal of Biological Macromolecules*, *318*, 145243. https://doi.org/10.1016/J.IJBIOMAC.2025.145243

Finger, C. A. G., Costa, E. A., Hess, A. F., Liesenberg, V., & Bispo, P. da C. (2023). Simulating Sustainable Forest Management Practices Using Crown Attributes: Insights for Araucaria angustifolia Trees in Southern Brazil. *Forests*, *14*(7), 1285. https://doi.org/10.3390/f14071285

Gómez-Bachar, L., Vilcovsky, M., González-Seligra, P., & Famá, L. (2024). Effects of PVA and yerba mate extract on extruded films of carboxymethyl cassava starch/PVA blends for antioxidant and mechanically resistant food packaging. *International Journal of Biological Macromolecules*, *268*, 131464. https://doi.org/10.1016/j.ijbiomac.2024.131464

Hoffmann, T. G., Angioletti, B. L., Bertoli, S. L., & de Souza, C. K. (2022). Intelligent pH-sensing film based on jaboticaba peels extract incorporated on a biopolymeric matrix. *Journal of Food Science and Technology*, *59*(3), 1001–1010. https://doi.org/10.1007/s13197-021-05104-6

Jorge, A. M. S., Gaspar, M. C., Henriques, M. H. F., & Braga, M. E. M. (2023). Edible films produced from agrifood by-products and wastes. *Innovative Food Science & Emerging Technologies*, *88*(4), 103442. https://doi.org/10.1016/j.ifset.2023.103442

Karnwal, A., Rauf, A., Jassim, A. Y., Selvaraj, M., Al-Tawaha, A. R. M. S., Kashyap, P., Kumar, D., & Malik, T. (2025). Advanced starch-based films for food packaging: Innovations in sustainability and functional properties. *Food Chemistry: X*, *29*, 102662. https://doi.org/10.1016/j.fochx.2025.102662

Kizil, R., Irudayaraj, J., & Seetharaman, K. (2002). Characterization of Irradiated Starches by Using FT-Raman and FTIR Spectroscopy. *Journal of Agricultural and Food Chemistry*, *50*(14), 3912–3918. https://doi.org/10.1021/jf011652p

Kupervaser, M. G., Traffano-Schiffo, M. V., Dellamea, M. L., Flores, S. K., & Sosa, C. A. (2023). Trends in starch-based edible films and coatings enriched with tropical fruits extracts: a review. *Food Hydrocolloids for Health*, *4*, 100138. https://doi.org/10.1016/J.FHFH.2023.100138

Mali, S., Grossmann, M. V. E., García, M. A., Martino, M. N., & Zaritzky, N. E. (2006). Effects of controlled storage on thermal, mechanical and barrier properties of plasticized films from different starch sources. *Journal of Food Engineering*, *75*(4), 453–460. https://doi.org/10.1016/j.jfoodeng.2005.04.031

Marafon, K., Carvalho, A. C. F., Prestes, A. A., de Souza, C. K., Andrade, D. R. M., Helm, C. V., Pereira, F. N., Tedeschi, P., de Gois, J. S., & Prudencio, E. S. (2025). Development and Characterization of Pinhão Extract Powders Using Inulin and Polydextrose as Prebiotic Carriers. *Processes*, *14*(1), 119. https://doi.org/10.3390/pr14010119

Marafon, K., Pereira-Coelho, M., da Silva Haas, I. C., da Silva Monteiro Wanderley, B. R., de Gois, J. S., Vitali, L., Luna, A. S., Canella, M. H. M., Hernández, E., de Mello Castanho Amboni, R. D., & Prudencio, E. S. (2024). An opportunity for acerola pulp (Malpighia emarginata DC) valorization evaluating its performance during the block cryoconcentration by physicochemical, bioactive compounds, HPLC–ESI-MS/MS, and multi-elemental profile analysis. *Food Research International*, *176*, 113793. https://doi.org/10.1016/j.foodres.2023.113793

Moreno, F. L., Raventós, M., Hernández, E., & Ruiz, Y. (2014). Block freeze-concentration of coffee extract: Effect of freezing and thawing stages on solute recovery and bioactive compounds. *Journal of Food Engineering*, *120*, 158–166. https://doi.org/10.1016/j.jfoodeng.2013.07.034

Mueller, E., Gabriela Hoffmann, T., Ferreira Carvalho, A. C., Meinert, C., Vieira Helm, C., Priyadarshi, R., & Krebs de Souza, C. (2025). Smart Biodegradable Packaging Film from Cassava Starch, Pea Flour, and Yerba Mate Extract. *Journal of Packaging Technology and Research*. https://doi.org/10.1007/s41783-025-00197-2

Mueller, E., Hoffmann, T. G., Schmitz, F. R. W., Helm, C. V., Roy, S., Bertoli, S. L., & de Souza, C. K. (2024). Development of ternary polymeric films based on cassava starch, pea flour and green banana flour for food packaging. *International Journal of Biological Macromolecules*, *256*, 128436. https://doi.org/10.1016/j.ijbiomac.2023.128436

Nolasco, A., Squillante, J., Velotto, S., D'Auria, G., Ferranti, P., Mamone, G., Errico, M. E., Avolio, R., Castaldo, R., De Luca, L., Romano, R., Esposito, F., & Cirillo, T. (2024). Exploring the Untapped Potential of Pine Nut Skin By-Products: A Holistic Characterization and Recycling Approach. *Foods*, *13*(7), 1044. https://doi.org/10.3390/foods13071044

Othman, S. H., Ronzi, N. D. A., Shapi'i, R. A., Dun, M., Ariffin, S. H., & Mohammed, M. A. P. (2023). Biodegradability of Starch Nanocomposite Films Containing Different Concentrations of Chitosan Nanoparticles in Compost and Planting Soils. *Coatings*, *13*(4), 777. https://doi.org/10.3390/coatings13040777

Pelissari, F. M., Sobral, P. J. do A., & Menegalli, F. C. (2014). Isolation and characterization of cellulose nanofibers from banana peels. *Cellulose*, *21*(1), 417–432. https://doi.org/10.1007/s10570-013-0138-6

Pérez-Bermúdez, I., Castillo-Suero, A., Jara-Leiva, C., Cortés-Valdivia, A., Rojas-Rojas, K., García-Rojas, V., Opazo-Navarrete, M., Guerra-Valle, M., Petzold, G., & Orellana-Palma, P. (2025). Effect of Block Freeze Concentration on Bioactive Compound Content and Antioxidant Capacity When Applied to Peppermint (Mentha Piperita L.) Infusion. *Antioxidants*, *14*(2), 129. https://doi.org/10.3390/antiox14020129

Prestes, A. A., Andrade, D. R. M., Canella, M. H. M., Haas, I. C. da S., Helm, C. V., de Gois, J. S., Block, J. M., Wanderley, B. R. da S. M., Amboni, R. D. de M. C., Cruz, A. G. da, Pimentel, T. C., & Prudencio, E. S. (2024). The Addition of Concentrated Cold-Pressed Guabiroba Juice to Yogurts: Effects on the Physicochemical Analyses, Antioxidant Activity, Carotenoid Content, Total Phenolic Compounds, and Mineral Profile. *Processes*, *12*(9), 1915. https://doi.org/10.3390/pr12091915

Prestes, A. A., Helm, C. V., Esmerino, E. A., Silva, R., da Cruz, A. G., & Prudencio, E. S. (2022). Freeze concentration techniques as alternative methods to thermal processing in dairy manufacturing: A review. *Journal of Food Science*, *87*(2), 488–502. https://doi.org/10.1111/1750-3841.16027

Prestes, A. A., Marafon, K., Carvalho, A. C. F., Andrade, D. R. M., Helm, C. V., de Gois, J. S., Monteiro Wanderley, B. R. da S., Amboni, R. D. de M. C., & Prudencio, E. S. (2024). The Functional Carbonated Beverage Properties of Guabiroba Juice Using the Ice Fraction from Gravitational Block Freeze Concentration. *Processes*, *12*(10), 2235. https://doi.org/10.3390/pr12102235

Priyadarshi, R., Ezati, P., & Rhim, J.-W. (2021). Recent Advances in Intelligent Food Packaging Applications Using Natural Food Colorants. *ACS Food Science & Technology*, *1*(2), 124–138. https://doi.org/10.1021/acsfoodscitech.0c00039

Priyadarshi, R., & Rhim, J. W. (2020). Chitosan-based biodegradable functional films for food packaging applications. *Innovative Food Science & Emerging Technologies*, *62*, 102346. https://doi.org/10.1016/J.IFSET.2020.102346

Ramírez, C., Gallegos, I., Ihl, M., & Bifani, V. (2012). Study of contact angle, wettability and water vapor permeability in carboxymethylcellulose (CMC) based film with murta leaves (Ugni molinae Turcz) extract. *Journal of Food Engineering*, *109*(3), 424–429. https://doi.org/10.1016/j.jfoodeng.2011.11.005

Re, R., Pellegrini, N., Proteggente, A., Pannala, A., Yang, M., & Rice-Evans, C. (1999). Antioxidant activity applying an improved ABTS radical cation decolorization assay. *Free Radical Biology and Medicine*, *26*(9–10), 1231–1237. https://doi.org/10.1016/S0891-5849(98)00315-3

Regmi, S., & Janaswamy, S. (2024). Biodegradable films from soyhull cellulosic residue with UV protection and antioxidant properties improve the shelf-life of post-harvested raspberries. *Food Chemistry*, *460*, 140672. https://doi.org/10.1016/j.foodchem.2024.140672

Sales, P. F. de, Silva, Y. R. de O., Lapa, L. S. S., & Amaral, F. H. C. (2021). Caracterização e aplicação de filmes biodegradáveis de amido de incorporados de extrato de própolis-verde. *ForScience*, *9*(2), e00958. https://doi.org/10.29069/forscience.2021v9n2.e958

Salvadori, N. M., da Conceição das Mercês, Z., Evangelista, S. M., Cochlar, T. B., de Oliveira Rios, A., & de Oliveira, V. R. (2024). Overview of the potential of pine nuts (Araucaria angustifolia) in new food options and films: an approach on quality, versatility and sustainability. *International Journal of Food Science and Technology*, *59*(10), 6916–6924. https://doi.org/10.1111/ijfs.17514

Sanchez, L. M., de Haro, J., Domínguez, E., Rodríguez, A., Heredia, A., & Benítez, J. J. (2024). Revalorization of Yerba Mate Residues: Biopolymers-Based Films of Dual Wettability as Potential Mulching Materials. *Polymers*, *16*(6), 815. https://doi.org/10.3390/polym16060815

Santhosh, R., Ahmed, J., Thakur, R., & Sarkar, P. (2024). Starch-based edible packaging: rheological, thermal, mechanical, microstructural, and barrier properties – a review. *Sustainable Food Technology*, *2*(2), 307–330. https://doi.org/10.1039/D3FB00211J

Sapper, M., Talens, P., & Chiralt, A. (2019). Improving Functional Properties of Cassava Starch-Based Films by Incorporating Xanthan, Gellan, or Pullulan Gums. *International Journal of Polymer Science*, *2019*, 1–8. https://doi.org/10.1155/2019/5367164

Sbruzzi Fiebig, M., Regina Mendes Andrade, D., José de Oliveira Mindelo, L., Santos de Gois, J., Luna, A. S., Afonso Provenzi, M., Luiz Esteves Magalhães, W., Miotto, M., Vieira Helm, C., & Schwinden Prudencio, E. (2024). Pinhão potential and their parts (failures, shells, and almonds) in the elaboration of yogurts containing acai pulp: physicochemical, nutritional, and functional properties, antimicrobial activity, and multi-elemental profile. *Food Research International*, *192*, 114813. https://doi.org/10.1016/j.foodres.2024.114813

Shahrim, N. A., Sarifuddin, N., Ahmad Azhar, A. Z., & Mohd Zaki, H. H. (2022). Biodegradation of Mango seed starch films in soil. *IIUM Engineering Journal*, *23*(1), 258–267. https://doi.org/10.31436/iiumej.v23i1.1620

Silveira Hornung, P., Ávila, S., Apea-Bah, F. B., Liu, J., Lopes Teixeira, G., Hoffmann Ribani, R., & Beta, T. (2020). Sustainable Use of Ilex paraguariensis Waste in Improving Biodegradable Corn Starch Films' Mechanical, Thermal and Bioactive Properties. *Journal of Polymers and the Environment*, *28*(6), 1696–1709. https://doi.org/10.1007/s10924-020-01723-w

Singh, P., Pandey, V. K., Singh, R., Singh, K., Dash, K. K., & Malik, S. (2024). Unveiling the potential of starch-blended biodegradable polymers for substantializing the eco-friendly innovations. *Journal of Agriculture and Food Research*, *15*, 101065. https://doi.org/10.1016/J.JAFR.2024.101065

Singleton, V. L., & Rossi, J. A. (1965). Colorimetry of Total Phenolics with Phosphomolybdic-Phosphotungstic Acid Reagents. *American Journal of Enology and Viticulture*, *16*(3), 144–158. https://doi.org/10.5344/ajev.1965.16.3.144

Sirbu, E.-E., Dinita, A., Tănase, M., Portoacă, A.-I., Bondarev, A., Enascuta, C.-E., & Calin, C. (2024). Influence of Plasticizers Concentration on Thermal, Mechanical, and Physicochemical Properties on Starch Films. *Processes*, *12*(9), 2021. https://doi.org/10.3390/pr12092021

Suh, J. H., Ock, S. Y., Park, G. D., Lee, M. H., & Park, H. J. (2020). Effect of moisture content on the heat-sealing property of starch films from different botanical sources. *Polymer Testing*, *89*, 106612. https://doi.org/10.1016/J.POLYMERTESTING.2020.106612

Suhag, R., Kumar, N., Petkoska, A. T., & Upadhyay, A. (2020). Film formation and deposition methods of edible coating on food products: A review. *Food Research International*, *136*, 109582. https://doi.org/10.1016/j.foodres.2020.109582

Uald-lamkaddam, I., Dadrasnia, A., Llenas, L., Ponsá, S., Colón, J., Vega, E., & Mora, M. (2021). Application of Freeze Concentration Technologies to Valorize Nutrient-Rich Effluents Generated from the Anaerobic Digestion of Agro-Industrial Wastes. *Sustainability*, *13*(24), 13769. https://doi.org/10.3390/su132413769

Usman, A., Hussain, Z., Riaz, A., & Khan, A. N. (2016). Enhanced mechanical, thermal and antimicrobial properties of poly(vinyl alcohol)/graphene oxide/starch/silver nanocomposites films. *Carbohydrate Polymers*, *153*, 592–599. https://doi.org/10.1016/j.carbpol.2016.08.026

Vilar-Bustillo, J., Ruiz-Rodríguez, A., Carrera, C. A., Piñeiro, Z., & Palma, M. (2023). Effects of Different Freezing Treatments during the Winemaking of a Varietal White Wine with Regard to Its Phenolic Components. *Foods*, *12*(10), 1963. https://doi.org/10.3390/foods12101963

Zhang, J., Liu, S., Xie, C., Wang, C., Zhong, Y., & Fan, K. (2024). Recent advances in pH-sensitive indicator films based on natural colorants for smart monitoring of food freshness: a review. *Critical Reviews in Food Science and Nutrition*, *64*(33), 12800–12819. https://doi.org/10.1080/10408398.2023.2257327

Zhang, Z., Tian, X., Wang, P., Jiang, H., & Li, W. (2019). Compositional, morphological, and physicochemical properties of starches from red adzuki bean, chickpea, faba bean, and baiyue bean grown in China. *Food Science & Nutrition*, *7*(8), 2485–2494. https://doi.org/10.1002/fsn3.865